

Influence of Chemisorption of Sulfite Ions on Electroreduction of Gold(I)–Sulfite Complexes

by G. Baltrūnas, A. Valiūnienė and R. Valiūnas

Department of Physical Chemistry, Vilnius University, Naugarduko 24, LT-2006 Vilnius, Lithuania, E-mail: gintaras.baltrunas@chf.vu.lt

(Received March 24th, 2003; revised manuscript July 15th, 2003)

Analysis of voltammograms, chronoamperograms and electrochemical impedance spectra (0.05–4000 Hz) indicate a slow stage of chemisorption of sulfite ions that reduces an active surface of gold electrode, and significantly influences a parallel stage of charge transfer of gold(I)–sulfite complexes. The proposed equivalent circuit representing electrochemical process well fits to experimental dependencies of real and imaginary parts of impedance on frequency. Values of elements of equivalent circuit at different potentials of gold electrode (0.1–0.5 V) were calculated. Cathodic voltammogram simulated by using the dependencies of elements of equivalent circuit on electrode potential rather well represents experimentally obtained voltammograms.

Key words: sulfite ions, chemisorption, gold(I)–sulfite complex, electroreduction, electrochemical impedance, equivalent circuit

High quality gold deposits having very low porosity can be obtained from gold(I)–sulfite baths [1]. This process can replace widely used gold-electroplating from cyanide baths. It is particularly useful for fabrication of micro technique devices, e.g. for the electroforming of absorber-structures on the masks used in X-ray deep lithography [2,3]. Despite the high interest in this process, most publications [4–6] deal with practical problems solely. Using cyclic voltammetry on the rotating disk electrode, the Shirai and co-workers [7] reported that the gold deposition processes from the gold(I)–sulfite bath consist of the three following steps with a charge-transfer as a rate-determining step: $\text{Au}(\text{SO}_3)_2^{3-} \rightarrow \text{AuSO}_3^- + \text{SO}_3^{2-}$; $\text{AuSO}_3^- \rightarrow \text{Au}^+ + \text{SO}_3^{2-}$; $\text{Au}^+ + \text{e}^- \rightarrow \text{Au}$.

Based on this mechanism and spectroscopic data obtained at high temperatures [8], the authors conclude that the disproportionation reaction in weakly alkaline solutions (pH 8) occurs: $3\text{Au}^+ \rightarrow 2\text{Au} + \text{Au}^{3+}$.

Applying voltammetry as an on-line analytical method in the gold(I)–sulfite bath [9], the unusually poor reproducibility of the data, namely the dependence of the current-potential curves on the value of the initial potential, and on the duration of the polarization at the initial potential was found. This suggests that the gold surface activity in sulfite-containing bath might be inhomogeneous. In the potential range more positive than –0.6 V the current density is independent of the rotation rate. The limiting current density (<–0.8 V) rises linearly with the square root of rotation frequency of the rotating disk electrode and is determined by the diffusion of $\text{Au}(\text{SO}_3)_2^{3-}$.

The diffusion coefficient value of the gold complex in the bath used was found as $7.6 \times 10^{-6} \text{ cm}^2 \text{ s}^{-1}$.

The previous study [10] on the stability of gold(I)–sulfite complexes by means of equilibrium gold potentials measurements did not give reliable results. The stability constant of gold(I)–sulfite complexes was determined as $\log \beta_2 \cong 28$ from the measurements of sparingly soluble gold(I) salts solubility in the solutions with various concentration of Na_2SO_3 . The similar value ($\log \beta_2 \cong 27.4$) was determined based on the measured potentials of gold amalgam [11]. Furthermore, in this work the attention was paid for unusual impedance spectra of gold electrode obtained in sulfite gold-plating baths. Namely, the imaginary part of impedance turned to positive values, while at some potentials the values of real part became negative. It is impossible to simulate such spectra by means of classical equivalent circuits.

The interaction of sulfite and products of its oxidation and reduction with surface of gold electrode and adsorption processes sometimes passivate the electrode surface [12–14]. Even the formation of elemental sulphur layer on electrode was observed [13]. This sulphur layer is stable only in some potential region. Noted, these investigations were carried out mostly in the more acidic solutions (pH 6) than solutions used in the present investigation (pH 9.5). However, the similar interaction is expected too, but probably weaker in other regions of potentials and in weakly alkaline solutions.

Therefore, in the present work an attempt has been made to design a new equivalent circuit, taking into account the interaction of electroreduction of gold(I)–sulfite complexes and chemisorption processes.

EXPERIMENTAL

The gold(I)–sulfite electrolyte was prepared from gold concentrate (IMABRITE 24, Schlötter, Germany), p. a. grade Na_2SO_3 and distilled water. All measurements were performed in an electrolyte of 0.05 M $\text{Au}(\text{SO}_3)_2^{3-}$, 0.5 M SO_3^{2-} of pH 9.5. Thicker gold layers were plated at 50°C, except where stated otherwise.

The experiments were carried out by using AMOS/ANDI IM5d measuring system (Zahner, Germany) with a regular 3-electrode cell. A Pt-wire of 0.5 mm \varnothing (0.157 cm^2) plated with a $10 \mu\text{m}$ gold layer from a sulfite bath before the measurements served as working electrode. The counter electrode was a Pt-mesh cylinder (20 cm^3) and the system $\text{Ag}|\text{AgCl}||3\text{M KCl}$ was used as the reference electrode.

All measurements were performed in nitrogen atmosphere. The potential values are referred to the standard hydrogen electrode (SHE). For the impedance measurements an AC-amplitude of 5 mV was used.

RESULTS AND DISCUSSION

Cyclic voltammetry and chronoamperometry. The shape of cyclic voltammogram obtained for electroreduction of the gold(I)–sulfite ions on the gold electrode is associated with the high electrode polarization and shows a complicated behaviour. In the reversed potential scan of the cyclic voltammogram (Fig. 1a), an additional horizontal section of the cathodic current density is obtained in the range of $-0.55 < E <$

-0.45 V. When rotating disk electrode was used, the current density increases at potentials higher than $E_H = -0.6$ V, but remains almost the same at lower polarization (Fig. 1b). In more detail it can be seen in Fig. 2a, where the initial region of the cyclic voltammogram is shown ($0.1 > E > -0.4$ V). In this region the current-potential curve has a maximum. Interestingly, that current density decreases with increasing of potential scan rate. Therefore, we can conclude that initial region of voltammogram is defined rather by slow charge transfer than mass transfer of gold complexes. In our opinion, this is probably caused by the time and potential dependent partial passivation of the electrode surface that influences on both kinetic and diffusion steps of the electroreduction. In this case, according to Matsuda theory [15], the sensible deflections should be obtained on the experimentally obtained chronoamperograms from predicted by Cottrell's equation: $-j = zFC_0D^{1/2}\pi^{-1/2}t^{-1/2}$, where C_0 – bulk concentration of diffusing species; zF – charge consumed by one mole of reactant; D – diffusion coefficient; t – deposition time. In accordance with Cottrell's equation, the rectilinear dependency should be obtained in the coordinates $-j$ vs. $t^{-1/2}$.

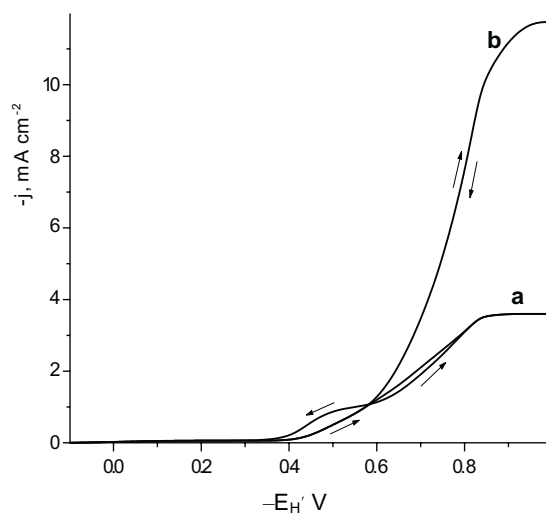


Figure 1. Cyclic voltammograms of electroreduction of the gold(I)-sulfite complex, $V = 2 \text{ mV s}^{-1}$. Composition of solution: $0.05 \text{ M Na}_3\text{Au}(\text{SO}_3)_2$, $0.5 \text{ M Na}_2\text{SO}_3$, pH 9.5. Electrode rotation rate, rad s^{-1} : a – 0; b – 24.

The comparison of experimental current transients and those simulated by Cottrell's equation is shown in Fig. 3. In this set of experiments the potential was changed from the initial value to the value corresponding to the diffusion limiting current (to $E = -0.85$ V). The initial potentials were in the range 0.1 to -0.5 V, where current density was negligible (see Fig. 1). Therefore, in course of potential steps the surface concentration of gold complexes changed from the approximately bulk value (C_0) to zero. Experimentally determined current transients differ from those theoretically calculated both in absolute values and shape. Only at $E_{\text{in}} = -0.45$ V or more negative, experimental and theoretical chronoamperograms are practically identical. When E_{in} are more positive, the differences between experimental and theoretical voltammo-

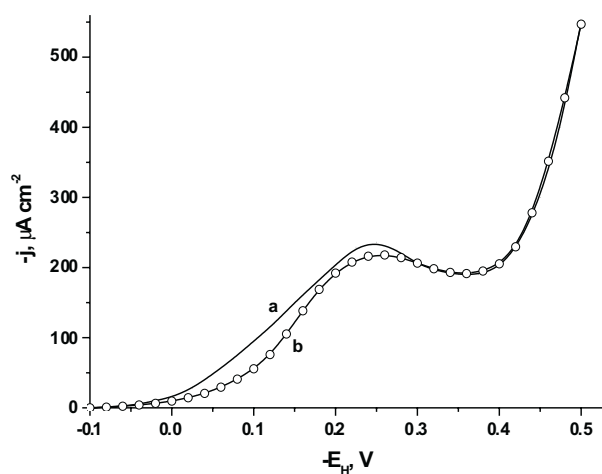


Figure 2. Initial section of voltammogram: a – experimentally obtained; b – simulated according to eq. (17). Solution composition as in Fig. 1.

grams are caused by passivation of the surface. According to the theory of diffusion to partially blocked surface of electrode [15] it should mean that at potentials -0.45 V or more negative a whole surface of electrode is active, or at least becomes active immediately after potential step is applied. Since the shape of chronoamperogram depends not on surface coverage degree (Θ) only, but also on geometry of active sites of electrode [15], consecutive alteration of chronoamperograms (Fig. 3 a–f) does not mean that Θ changes in the same manner. Passivation model of process is also proved by chronoamperometric measurements in the same solution and under the same condi-

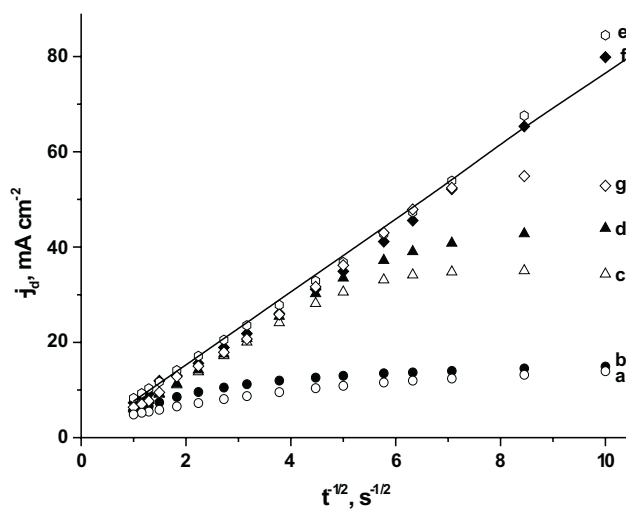


Figure 3. Chronoamperograms of the electroreduction of the gold(I)–sulfite complex onto gold (a–f) and silver (g) electrodes. Step potential (all) -0.85 V, initial potential: 0.10 V (a, g); 0.0 V (b); -0.15 V (c); -0.3 V (d); -0.45 V (e); -0.5 V (f). The line labeled “ j_d ” was calculated from Cottrell equation.

tions as in Fig. 3a, but on silver electrode instead of gold. This chronoamperogram conforms with theoretical one (Fig. 3g), while small discrepancies at shortest times can be explained by slow electrocrystallization of gold on silver electrode.

After a potential step of any magnitude is applied, usually current decreases within first 10–20 sec, then a constant current density is established, due to natural convection. After applying potential step from equilibrium potential to -0.7 V in investigated bath discussed above, exactly this kind of current change is observed (Fig. 4). However, the shapes of chronoamperograms are quite different at lower magnitudes of polarization: within 4–6 sec after potential step current decrease is finished, then current begins to increase instead remains at constant level. It can be explained only by increased active surface of electrode. Since this current change lasts for 200–300 sec, we can conclude that adsorption – desorption process of sulfite ions or their derivatives is extremely slow. Even more complicated chronoamperogram is observed when 0.4 V potential is applied to electrode: within first 20 seconds current increases, then begins to decrease. Probably in this potential region contents or structure of adsorption layer and after establishing of equilibrium active surface of electrode can be even smaller than active surface at equilibrium potential.

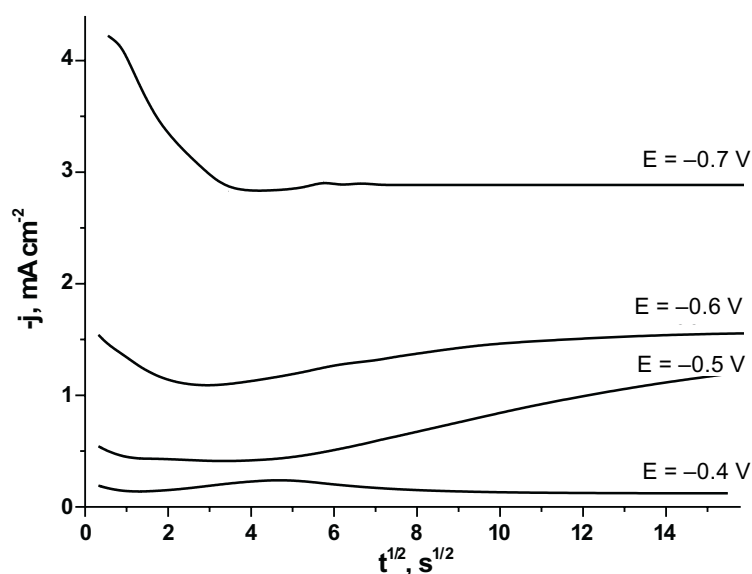


Figure 4. Chronoamperograms of the electroreduction of the gold(I)–sulfite complex. Initial (equilibrium) potential 0.10 V, step potentials are marked above curves.

Electrochemical Impedance Spectroscopy. The qualitative analysis of the voltammograms in the presence of passivation is quite complicated, and further studies of gold electroreduction kinetics were studied by means of electrochemical impedance spectroscopy. The complicated voltammetric behavior of investigated system should

be reflected also on the Nyquist plots obtained at various electrode potentials. The impedance spectra were recorded in the frequency range of 0.05 to 4000 Hz, and are shown in Fig. 5.

Assuming a partial passivation model, the maximal blocking of the surface should be expected in the potential region of the current minimum (Fig. 2a, $E = -0.3 \div -0.4$ V). Therefore [16,17], electrochemical impedance spectra in the infra-low frequency domain may show positive values of the imaginary part and reach negative values of the real part at the potentials of the minimum current ($-0.25 > E > -0.35$ V).

At cathodic polarization $E = 0.1 \div -0.15$ V, Z' values are positive and Z'' are negative in the entire range of frequencies applied, and absolute values sequentially decrease (Fig. 5, a–d). When cathodic polarization increases up to $E = -0.2 \div -0.25$ V, the EIS begin to “unbend” increasing Z'' values (Fig. 5, e–f) to such a degree that at potentials more negative than -0.25 V the real part becomes negative (Fig. 5, g–i). At further cathodic polarization ($E < -0.4$ V), the real part of the impedance reaches positive values again and reflects more rapid decrease of the charge transfer resistance (Fig. 5, j–k). Noted, that the electroreduction rate (and probably, the state of the surface too) reproduces poorly. The course of the single observed dependency may vary by ± 50 mV from one experiment to another. In addition, after the potential step is applied, the components of the impedance reach constant values relatively slow. Therefore, the impedance spectra (Fig. 5) were recorded after polarizing for at least 60 min.

Usually, the electrochemical behaviour of the system can be simulated and quantified with equivalent electric circuits. Typical electric circuit (Fig. 6) assuming elec-

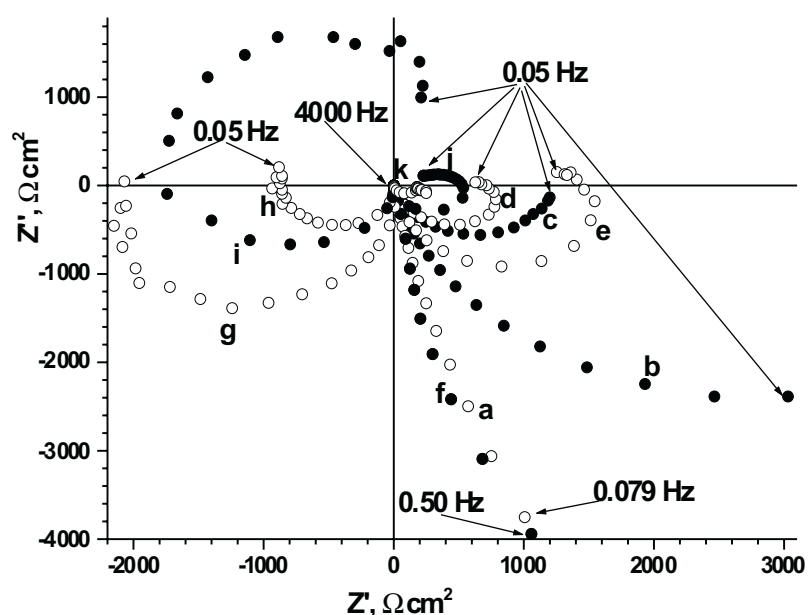


Figure 5. Impedance spectra obtained at different electrode potentials: 0.10 V (a), 0.00 V (b), -0.10 V (c), -0.15 V (d), -0.20 V (e), -0.25 V (f), -0.30 V (g), -0.35 V (h), -0.40 V (i), -0.45 V (j), -0.50 V (k).

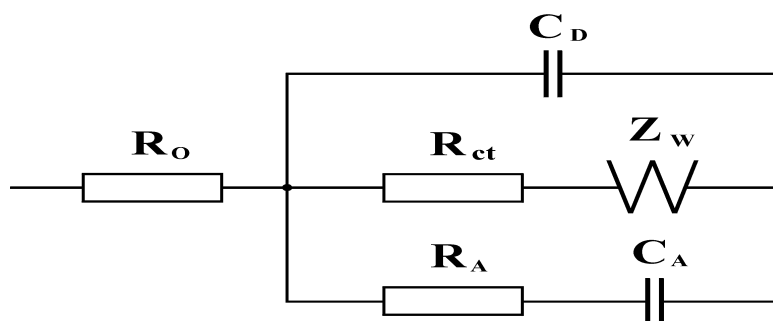


Figure 6. Electrical equivalent circuit. R_A and C_A are resistance and capacitance, which account for the adsorption/desorption processes. R_{ct} and C_D are the charge transfer resistance and the double layer capacitance, R_0 represents the uncompensated electrolyte resistance and Z_W is the Warburg impedance.

troreduction of complexes with parallel chemisorption of ligands [18] cannot describe obtained impedance spectra. Probably the reason is that influence of adsorption on electroreduction of complexes is not encountered in this scheme. The equivalent circuit should be modified under assumption that charge transfer resistance (R_{ct}) simulates $\text{Au}(\text{SO}_3)_2^{3-}$ electroreduction only on the surface area free of adsorbate (*i.e.* on the part $1 - \Theta$), and this area depends on the electrode potential. Since such model was not reported before, we will describe it more detailly.

Model. Firstly, the dependence of active part of electrode surface on electrode potential should be evaluated. To achieve this goal, we will use the method of complex amplitudes [19]. Further in this text complex amplitudes (phasors) of any variable are marked with hollow points as a superscript, *e.g.*, $Y^\circ = Y_0 \exp(j\psi)$, where ψ represents the phase shift with regard to factor causing alternation (in our case – potential), Y_0 is amplitude and j – imaginary unit [19].

Adsorption current passing through an electrochemical circuit can be expressed as

$$i_A = \frac{dq}{dt} = q_A \frac{dA}{dt}$$

where A – amount of adsorbed material (mol),

$$q_A = \left(\frac{\partial q}{\partial A} \right)_E$$

is charge transferred by 1 mol of adsorbed material. Thus complex amplitude of adsorption current can be expressed as follows:

$$I_A^\circ = j\omega q_A \Delta A^\circ \quad \text{or} \quad \Delta A^\circ = \frac{I_A^\circ}{q_A j\omega} \quad (1)$$

Total adsorption impedance [13] is expressed:

$$Z_A = R_A + \frac{1}{C_A j\omega} = \frac{1 + C_A R_A j\omega}{C_A j\omega} \quad (2)$$

where C_A and R_A are adsorption capacity and adsorption resistance, respectively. Then, the following expression is valid for complex amplitude of adsorption current:

$$I_A^\circ = \frac{\Delta E^\circ}{Z_A} = \frac{\Delta E^\circ C_A j\omega}{1 + C_A R_A j\omega} \quad (3)$$

Combining (3) with (1) yields:

$$\Delta A^\circ = \frac{\Delta E^\circ C_A j\omega}{q_A j\omega(1 + C_A R_A j\omega)} = \frac{\Delta E^\circ C_A}{q_A + q_A C_A R_A j\omega} = A_\infty \Theta^\circ \quad (4)$$

where A_∞ is maximum amount of adsorbed material on surface, $\Theta = A/A_\infty$ is degree of surface coverage by adsorbate. The charge required to cover the entire surface by adsorbate is expressed as $q_\infty = q_A A_\infty$. Then, the expression for complex amplitude of coverage degree we can derive from (4):

$$\Theta^\circ = \frac{\Delta E^\circ C_A}{q_A A_\infty(1 + C_A R_A j\omega)} = \frac{\Delta E^\circ C_A}{q_\infty(1 + C_A R_A j\omega)} \quad (5)$$

Next step is to evaluate the influence of active area oscillation on stage of electroreduction of Au(I)–sulfite complexes. In this stage the instant charge transfer current at partially covered electrode can be expressed as a function of both real current density

$$\left(I_{ct} = I_0 \exp\left(\frac{\alpha z F}{RT} \Delta E\right) \right)$$

and surface coverage (Θ) variables:

$$I(t) = I_{ct}(1 - \Theta) = I_{ct} - I_{ct}\Theta \quad (6)$$

and in differential form:

$$\frac{\partial I}{\partial t} = \frac{\partial I_{ct}}{\partial t} - \Theta \frac{\partial I_{ct}}{\partial t} - I_{ct} \frac{\partial \Theta}{\partial t} \quad (7)$$

Then the complex amplitude of current density is expressed:

$$I^\circ = \Delta E^\circ \left[\frac{\partial I_{ct}}{\partial E} (1 - \Theta) - \frac{\partial \Theta}{\partial E} I_{ct} \right] - I_{ct} \Theta^\circ \quad (8)$$

If term in angle brackets is marked as R_B^{-1} , by using (5) expression we can write:

$$I^{\circ} = \frac{\Delta E^{\circ}}{R_B} - I_{ct} \Theta^{\circ} = \frac{\Delta E^{\circ}}{R_B} - I_{ct} \frac{\Delta E^{\circ} C_A}{q_{\infty} (1 + C_A R_A j\omega)} \quad (9)$$

Having the complex amplitude of charge transfer we can also express the impedance of this stage:

$$Z = \frac{\Delta E^{\circ}}{I^{\circ}} = \frac{1}{\frac{1}{R_B} - \left(\frac{q_{\infty}}{I_{ct} C_A} + j\omega \frac{q_{\infty} R_A}{I_{ct}} \right)^{-1}} \quad (10)$$

For impedance of equivalent circuit (Fig. 7) consisting of two resistances (R_1 and R_2) and inductivity (L) the following expression is valid:

$$Z = \frac{1}{\frac{1}{R_1} + (R_2 + Lj\omega)^{-1}} \quad (11)$$

Considering

$$R_1 = R_B, \quad R_2 = R_L = -\frac{q_{\infty}}{I_{ct} C_A} \quad \text{and} \quad L = -\frac{q_{\infty} R_A}{I_{ct}},$$

expression (11) becomes identical with (10).

It proves that charge transfer resistance turns to circuit with inductivity shown in Fig. 7, if competitive reversible adsorption occurs. The origin of inductivity is caused by the finite rate of sulfite adsorption-desorption process (V_0), because according [19] to:

$$R_A = \frac{RT}{q_A^2 V_0} \quad (12)$$

Thus, the slower is the adsorption process, the larger is the influence of inductivity on charge transfer stage:

$$L = -\frac{q_{\infty}}{I_{ct}} \frac{RT}{q_A^2 V_0} = -RT \frac{A_{\infty}}{I_{ct} q_A V_0} \quad (13)$$

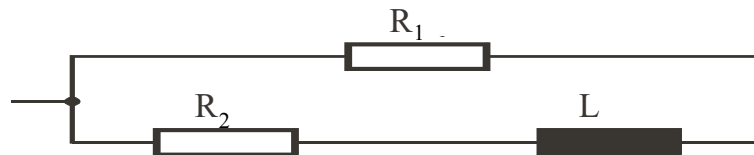


Figure 7. Electrical equivalent circuit. R_1 and R_2 – resistance, L – inductance.

Effects causing appearance of inductivity should be discussed separately. Larger R_A represents a slower adsorption. Phase of current, passing through circuit $R_A C_A$ overruns the phase of potential from 0 (slow adsorption) to $\pi/2$ (fast adsorption). Changes of amount of adsorbed species ΔA and surface coverage $\Delta \Theta$ are proportional to the integral of adsorption current passed, *i.e.* their phases lag behind I_A by $\pi/2$. Thus, phase of $\Delta \Theta$ lags behind phase of potential from $\pi/2$ (slow adsorption) to 0 (fast adsorption). In present model potential is more negative than equilibrium potential, thus small constant current (I_{ct}) passes through system. Alternating of surface coverage should cause alternation of this current with lagging phase shift with regard to potential from $-\pi/2$ (adsorption slow) to 0 (adsorption fast), what is characteristic feature of systems with resistance and inductivity. Obviously in absence of constant current or in the case of fast adsorption this circuit should be eliminated. Equation (13) describes that quantitatively.

The resistance R_B might have positive or negative values. According to definition for R_B :

$$R_B = \left[\frac{\partial I_{ct}}{\partial E} (1 - \Theta) - \frac{\partial \Theta}{\partial E} I_{ct} \right]^{-1} \quad (14)$$

Since cathodic current always is negative $I_{ct} < 0$, and $\partial I_{ct} / \partial E > 0$, *i.e.* the first term of this equation is always positive, we can distinguish several options:

$$\begin{aligned} \text{when } \frac{\partial \Theta}{\partial E} > 0, \quad \text{then } R_B > 0 \quad \text{in all cases} \\ \text{when } \frac{\partial \Theta}{\partial E} < 0, \quad \text{then } R_B > 0, \quad \text{if } \frac{\partial I_{ct}}{\partial E} (1 - \Theta) > \frac{\partial \Theta}{\partial E} I_{ct}, \\ \quad \quad \quad \text{and } R_B < 0, \quad \text{if } \frac{\partial I_{ct}}{\partial E} (1 - \Theta) < \frac{\partial \Theta}{\partial E} I_{ct} \end{aligned} \quad (15)$$

Therefore, R_B can rise to negative values when potential sweep to negative values causes enough rapid coverage of electrode surface by adsorbate, and electroreduction of complexes is fast enough too. From magnitudes of R_B given in Table 1 one can see that at potential $E_H = -0.25$ V equity

$$\frac{\partial I_{ct}}{\partial E} (1 - \Theta) \cong \frac{\partial \Theta}{\partial E} I_{ct}$$

is valid, whereas in potential region $-0.25 \text{ V} \geq E_H \geq -0.4 \text{ V}$ valid is

$$\frac{\partial I_{ct}}{\partial E} (1 - \Theta) < \frac{\partial \Theta}{\partial E} I_{ct}$$

Under assumption, that all adsorbed sulfite ions reduce the active area of electrode thereby influencing on the electroreduction of gold–sulfite complexes, according to definitions for R_C and L by (Eq. 10) the following condition should be valid:

$$\frac{L}{R_C} = R_A C_A \quad (16)$$

Analysis of impedance spectra. The experimental impedance data were analysed in the frame of modified equivalent circuit (Fig. 8). We replaced the charge transfer resistance R_{ct} in the typical circuit (Fig. 6) by circuit including inductivity (Fig. 7). Diffusion impedance Z_W (Fig. 6) was not encountered because in the range of frequencies applied did not exceed $1 \div 2 \Omega \text{ cm}^2$, whereas circuit elements consequent to Z_W reached hundreds and thousands of ohms.

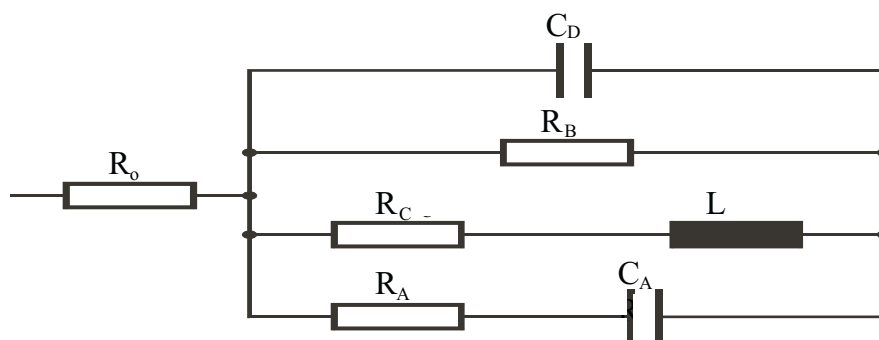


Figure 8. Electrical equivalent circuit for process of electroreduction of gold(I)–sulfite complexes complicated by chemisorption of sulfite ions. Marking of elements the same as in Fig. 6 and Fig. 7.

Values of parameters calculated from experimental impedance spectra (Fig. 5) by the use of equivalent circuit represented in Fig. 8 are listed in Table 1. Dashes in this Table mean that at some potentials impedance of circuit $R_C L$ is so huge, in comparison with parallel to $R_C L$ elements of circuit, that reliable determination of these parameters is impossible. As one can see from the results of analysis, uncompensated resistance of solution ($0.72 \pm 0.2 \Omega \text{ cm}^2$) is significantly less than other parameters and can influence total impedance only at high frequencies. The dependence of other parameters of circuit on electrode potential is complicated and requires additional study. As it was expected, based on the shape of impedance spectra, parameter R_C is negative in the potential range -0.3 to -0.4 V. As it was mentioned above, it can happen only when more negative potential increases the degree of surface coverage in contrary to the classical case of anion chemisorption. Therefore, it is complicated to explain this phenomenon. Probably, the adsorption of sulfite ions occurs in few steps: first is fast and transfers big amount of charge (it is represented by circuit $R_A C_A$), and second step is slow and related with regrouping of adsorbed ions (charge transfer can be negligible). Exactly, the products of second adsorption stage probably influence the electroreduction of gold(I)–sulfite complexes. This hypothetical mechanism can explain why calculated parameters of equivalent circuit do not fit equation (16).

Fig. 9 shows rather good agreement between the simulated and measured frequency dependencies of the impedance. Simulated frequency dependencies of the impe-

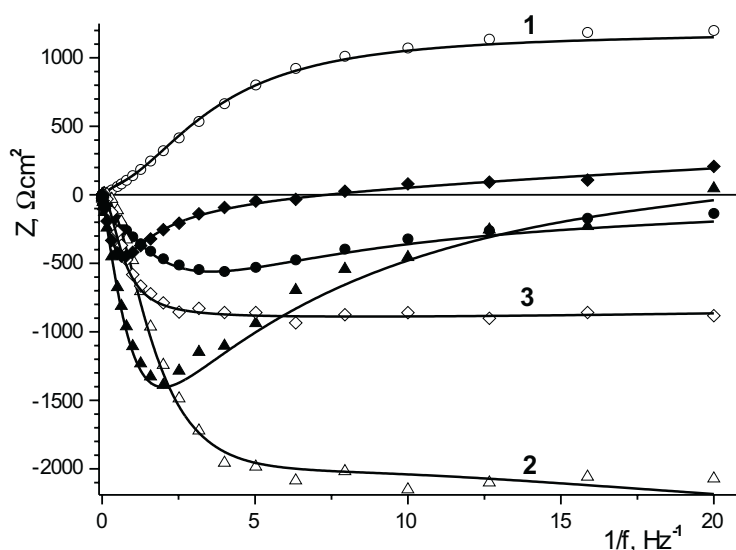


Figure 9. Experimentally obtained dependencies of real (hollow symbols) and imaginary (filled symbols) impedance's components on frequency, and simulated in accordance with equivalent circuit (Fig. 8). Values of elements from Table 1. Potential of electrode: -0.1 V (1); -0.3 V (2); -0.35 V (3).

dance have been obtained according to the equivalent circuit (Fig. 8), where the values of the elements are listed in Table 1.

Table 1. Values of parameters of equivalent circuit (shown in Fig. 6) calculated by using electrochemical impedance spectra (shown in Fig. 3).

No	E_H V	R_0 $\Omega \text{ cm}^2$	C_D $\mu\text{F cm}^{-2}$	R_A $\Omega \text{ cm}^2$	C_A $\mu\text{F cm}^{-2}$	R_B $\Omega \text{ cm}^2$	R_C $\Omega \text{ cm}^2$	L H cm^2
1	0.1	0.82	352	3007	149	22260	–	–
2	0.0	0.81	286	752	204	4808	–	–
3	-0.1	0.75	267	320	191	1184	–	–
4	-0.15	0.70	189	45.7	130	853	2048	3550
5	-0.2	0.65	114	42.5	56	1848	2434	2940
6	-0.25	0.74	44.8	91.7	30.8	29712	34000	100
7	-0.3	0.76	90.6	121	825	-913	1495	2050
8	-0.35	0.62	84.4	9.1	36.6	-881	949	11000
9	-0.4	0.57	67.8	7.52	17.3	-1421	722	704
10	-0.45	0.92	33.7	0.665	2.34	547	580	306
11	-0.5	0.55	58.4	18.8	18.7	183	–	–

To check adequacy of model assumed to studied electrochemical system the voltammograms were used (Fig. 2a). When potential scan rate is minimal, the constant current which passes through the system might be expressed:

$$j = I_{ct} (1 - \Theta) = \int_{E_0}^E \left(\frac{1}{R_B} + \frac{1}{R_C} \right) dE \quad (17)$$

In order to simulate a voltammogram, eq. (17) was digitally integrated using values R_B and R_C reported in Table 1. In the case of dashes, the value $1/R_C = 0$ was used. The simulated voltammogram shown in Fig. 2b is compared with voltammogram experimentally obtained at $V = 0.1$ mV/s. There is a good correlation between these voltammograms.

CONCLUSIONS

The slow chemisorption of sulfite ions takes place parallel to the reduction of gold(I)–sulfite complexes. The chemisorption influences strongly the charge transfer step of electroreduction complexes by reducing the active surface area of electrode. Due to this influence, both maximum of cathodic current appears in voltammograms and components of impedance turn to non-typical values, namely negative real part and positive imaginary part. A modelling of electrochemical system enables us to conclude, that circuit consisting of two resistances and inductivity instead of only one charge transfer resistance represents charge transfer reaction. Furthermore, one of these resistances can assume both positive and negative values.

Values of elements of equivalent circuit at different potentials (0.1÷–0.5 V) of gold electrode were calculated. Using dependencies of equivalent circuit elements on potential of electrode cathodic voltammograms were simulated. These voltammograms are in good agreement with experimentally obtained.

REFERENCES

1. Morrissey R.J., *Plating*, **80**, 75 (1993).
2. Dauksher W.J., Resnick D.J., Resnick W.A. and Yanof A.W., *Microelectronic Engineering*, **23**, 235 (1994).
3. Ehrfeld W. and Lehr H., *Radiat. Phys. Chem.*, **45**, 349 (1995).
4. Gemmler A., Keller W., Richter H. and Ruess K., *Metalloberfläche*, **47**, 461 (1993).
5. Okinaka J. and Hoshino M., *Gold Bull.*, **31**, 3 (1998).
6. Löwe H., Mensinger H. and Ehrfeld W., *Oberflächentechnik*, **50**, 77 (1994).
7. Shirai N., Yoshimura S., Sato E. and Kubota N., *J. Sur. Finish. Soc. Jpn.*, **40**, 543 (1989).
8. Honma H. and Hagiwara K., *J. Electrochem. Soc.*, **142**, 81 (1995).
9. Küpper M., Baltrunas G. and Löwe H., *Galvanotechnik*, **88**, 2906 (1997).
10. Pechewitskij B.J. and Erenburg A.M., *Izv. Sib. Otdel. AN SSSR, Ser. Khim. Nauk*, **4**, 24 (1976) (in Russian).
11. Baltrunas G., *Chemija (Vilnius)*, **10**, 112 (1999).
12. Varga K., Baradlai P. and Vertes A., *Electrochim. Acta*, **42**, 1143 (1997).
13. Fanigliulo A. and Bozzini B., *Trans IMF*, **80**, 132 (2002).
14. Westbroek P., De Strycker J., Van Uytfanghe K. and Temmerman E., *J. Electroanal. Chem.*, **516**, 83 (2001).
15. Gueshi T., Tokuda K. and Matsuda H., *J. Electroanal. Chem.*, **89**, 247 (1978).
16. Macdonald J.R., *Impedance Spectroscopy*, John Wiley & Sons, NY, 1987.
17. Deslouis C., Gabrielli C., Keddani M., Khalil A., Rosset R., Tribollet B. and Zidoune M., *Electrochim. Acta*, **42**, 1219 (1997).
18. Baltrunas G., Popkirov G.S. and Schindler R.N., *J. Electroanal. Chem.*, **435**, 95 (1997).
19. Grafov B.M. and Ukshe E.A., *The Electrochemical AC Circuits*, Nauka, Moscow, 1973 (in Russian).